Wojcieszak, D., Domaradzki, J., Pokora, P., Sikora, M., Mazur, M., Chodasewicz, P., Morgiel, J., & Gibson, D. (2022). Optical and structural properties of gradient (Ti,Co)Ox thin-film coatings with a resistive switching effect. *Applied Optics*, *61*(34), 10283-10289. https://doi.org/10.1364/AO.476918

*To be published in Applied Optics:*

**Title:** Optical and structural properties of gradient (Ti,Co)Ox thin-film coatings with resistive switching effect

**Authors:** Damian Wojcieszak,Jaroslaw Domaradzki,Patrycja Pokora,malwina sikora,Michal Mazur,Pawel Chodasewicz,Jerzy Morgiel,Des Gibson

**Accepted:** 07 November 22

**Posted** 09 November 22

**DOI:** https://doi.org/10.1364/AO.476918

# Optical and structural properties of gradient (Ti,Co)Ox thin-film coatings with resistive switching effect

DAMIAN WOJCIESZAK,[1,*] JAROSŁAW DOMARADZKI,[1] PATRYCJA POKORA,[1] MALWINA SIKORA, [1,2] MICHAŁ MAZUR,[1] PAWEŁ CHODASEWICZ,[1] JERZY MORGIEL,[3] DES GIBSON,[4,]

[1] *Wroclaw University of Science and Technology, Faculty of Electronics, Photonics and Microsystems, Janiszewskiego 11/17, 50-372 Wroclaw, Poland*
[2] *Nanores Company, Bierutowska 57-59, 51-317 Wroclaw*
[3] *Institute of Metallurgy and Materials Science of Polish Academy of Sciences, Reymonta 25 Str., 30-059 Krakow, Poland*
[4] *Institute of Thin Films, Sensors and Imaging, School of Engineering and Computing, University of the West of Scotland, PA1 2BE Paisley, Scotland, UK*
**damian.wojcieszak@pwr.edu.pl*

**Abstract:** In this work, the optical and structural properties of gradient (Ti,Co)Ox coatings with resistive switching effect have been outlined. They were prepared using multimagnetron sputtering and, despite the high cobalt content, they were transparent and had a high refractive index. Gradient Co-addition resulted in the receiving fine crystalline $TiO_2$ – anatase and $Co_3O_4$ forms in the amorphous surrounding. Observed resistance switching was a fully repeatable effect, and its occurrence in gradient (Ti,Co)Ox coatings was not reported earlier. The prepared gradient coatings exhibit great potential as transparent electronic devices with resistance switching effect. Such memory effects in transparent thin-film coatings open up new possibilities for the manufacturing of innovative memory elements in the future.





## 1. Introduction

Optical coatings based on metal oxides have been known and used for many years, especially in optics and optoelectronics. Currently, they are very popular in transparent oxide electronics, where various types of transparent electronic components can be produced on their basis. In the last decade, there has also been a lot of interest from various research groups in structures with resistive switching (RS) effect. However, the current state of the knowledge in the field of their operation is still insufficient that limits their application in practice [1-9]. Resistive switching devices are usually made on the basis of multilayers of various transparent metal oxides [10-12], therefore reports on the application of single gradient thin films in the construction of an RS device as an active layer instead of a typical multilayer stack is a new idea that has already been presented in our previous works [3,5]. It should also be noted that the gradient layers themselves are not commonly used today, especially in the construction of optical coatings. One of the most commonly used materials in the construction of optical coatings is titanium dioxide, of which many advantages and possibilities are already known [13-15]. It is also a good matrix for other elements, including cobalt. Cobalt oxides are one of the most studied oxides due to their importance in various fields such as supercapacitors, electrochromic sensors, solar selective absorbers, and energy storage devices [16-18]. In general, cobalt oxide can appear in three well-known forms: cobalt oxide (CoO), cobaltic oxide ($Co_2O_3$), and cobaltosic oxide ($Co_3O_4$). $Co_3O_4$ is especially interesting due to the p-type of electrical conduction and behaves like an antiferromagnetic (AF) with a Neel temperature $T_N$ of 290 K, it has a multiple direct band gap (2.28 eV, 1.57eV) [17-20]. The advantages briefly mentioned here have not yet been fully exploited. A literature review shows that materials based on (Ti,Co)Ox have not been well described in the literature so far. This is due to the fact that these types of oxide mixtures are usually in the form of nanotubes, nanowires, nanorods or nanoparticles, while thin films are a minority [13,14,16-23]. Usually, the amount of cobalt in the titanium dioxide matrix does not exceed 15 at.%, which in the case of thin films is associated with a significant reduction of their transparency above that content. The classification of oxide materials based on Ti and Co mixtures is difficult to reliably perform because of the dominant influence of the technology of their preparation. The key factor is the influence of the manufacturing method on the structure [18]. In the case of coatings, the preparation of crystalline ones usually requires additional annealing [13,14]. Without heat treatment or with a low deposition temperature, amorphous films can be received [15,16]. For this reason, the use of such mixed oxides in modern transparent electronics, where organic substrates are often used, indicates their high application potential. In this work, the optical and structural properties of gradient (Ti,Co)Ox coatings with a resistive switching effect are outlined. The films were prepared using multi-magnetron sputtering. The films obtained were transparent, and their structure changed from rare amorphous to fine nanocrystalline with an amorphous surrounding. As a result of the aforementioned high transparency, their use in optical coatings technology seems to be a chance to initiate work on a new type of transparent oxide electronic elements with memory properties.

## 2. Experimental

### *2.1. Preparation of the coatings*

Gradient (Ti,Co)Ox thin-film coatings were prepared using the multimagnetron sputtering system. Ti (99.95 %) and Co (99.95 %) metal discs (28 mm diameter and 3 mm thick) were simultaneously co-sputtered in a reactive oxide mode. Pre-cleaning of the surfaces of targets and substrates was applied (low-pressure plasma discharge in the chamber: AC supply, 170 W, $1.2\times10^{-1}$ mbar, 3 min.). The deposition processes were carried out using a mixture of Ar:$O_2$ (1:1) as a working and reactive gas. The constant flow of each gas was set during the entire deposition process at 8.4 sccm and was controlled by PR4000B (MKS) mass flow controllers. The films were deposited simultaneously on three types of substrates, $SiO_2$, Si and Ti4Al6V, positioned in a confocal configuration with respect to sputtered targets at a distance of 160 mm. The choice of different substrates results from the requirements. For magnetrons powering two separate 2 kW pulsed DC power supplies from Dora Power Systems were used [23-26]. To obtain a gradient concentration of Ti and Co elements versus film thickness, the magnetron equipped with the Ti target was powered with constant power fixed at 400 W, whereas the magnetron with the Co target was powered with a power that increased linearly from 0 W to 50 W. The total time of deposition was 240 min, which resulted in 370 nm of (Ti,Co)Ox thin film. Furthermore, to ensure the desired powering profile of magnetron equipped with a Co target, an own-made microcontroller was used [23,24]. During the deposition, no additional heating or electrical biasing was applied. Pressure during deposition was kept at about $2\cdot10^{-2}$ mbar. Details of the deposition process are collected in Table 1. To allow electrical tests, circular 1 mm Au pads were evaporated at the top of the (Ti,Co)Ox thin film deposited on the Ti6Al4V substrate.

### *2.2. Characterization of the films*

The surface and morphology observations at thin film cross section were performed with the use of a FEI Helios NanoLab 600i SEM coupled with an EDS spectrometer. Comparison of the intensity of CoKα and TiKα emission lines allowed the amount of each element to be determined. Electrical properties were determined based on DC current-voltage electrical measurements using a Keithley SCS4200 semiconductor characterization system (Keithley Instruments LLC) and an M100 probe station (Cascade Microtech). The optical properties of the gradient coatings were determined on the basis of transmission and reflection characteristics registered with the aid of OceanOptics scientific grade QE65000 optical spectrophotometer and a coupled deuterium-halogen lamp as a light source. In addition, also an Aquila NKD-8000 spectrophotometer was used for transmission measurements. Spectra were recorded for the 30° angle of incident light for S and P polarization. On their base, the refractive index (*n*) and extinction coefficient (*k*), as well as optical band gap ($E_g^{opt}$) were determined with the aid of Scout ver. 4.17 software [27]. Characterization of structural properties was performed on the basis of X-ray diffraction (XRD) results. The Empyrean PIXel3D diffractometer from Panalytical was used for pattern registration. The apparatus was operating in the grazing incidence mode (set at a 3 ° angle), with a Cu source. The 2theta scans were collected in the 20 ° - 80 ° range with a step size and a time of 0.05 ° and 2 s, respectively. The recorded patterns were analyzed with the aid of MDI JADE ver. 5.0 software. For Raman spectroscopy, a Thermo Scientific DXR™ Raman microscope was used. The studies were performed in the range from 100 to 1000 cm$^{-1}$ using a 455 nm blue laser diode as an excitation source and a 100x objective. The power of a light source was equal to 1 mW to avoid additional heating of the sample, which could result in a change of microstructure, e.g., crystallization of the gradient coating. Microstructure analysis has been extended to transmission electron microscopy studies. For measurements a TECNAI G2 FEG Super-Twin (200 kV) transmission (TEM) and scanning electron (SEM) microscope was used. For research purposes of TEM, high-quality lamellas were prepared using a focused-ion beam (FIB Quanta 3D system) equipped with an Omniprobe lift-out system. The Co-gradient as a function of the film depth was analyzed with a TEM-integrated X-ray energy dispersive attachment (EDS) with an EDAX UTW detector.

## 3. Results and discussion

In Fig. 1. EDS maps of the elemental distribution of the prepared gradient (Ti,Co)Ox coating are shown. As can be seen, the attached maps of O, Ti, and Co indicate a homogeneous distribution of each element. The total relative content was found to be 66.40 at.% of Ti and 33.60 at.% of Co. It should be noted that this result is averaged over the entire volume of the coating and does not contradict the fact that cobalt has a gradient distribution as a function of the thin-film depth. The SEM studies also confirmed the homogeneity of the film microstructure (Fig. 2). As can be seen from images of surface topography or the cross section of the coating, the densely packed, columnar structure has been obtained. Near the Si substrate, where the cobalt content is the lowest, the growth of the coating had a different nature than in the areas closer to the surface, where its amount gradually increased.

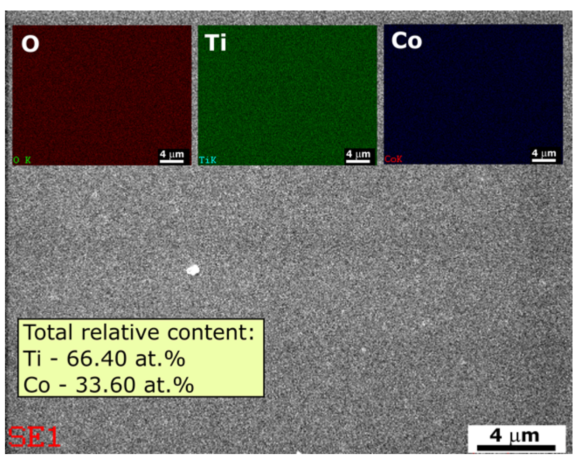


Fig. 1. EDS maps of the elemental distribution of the gradient (Ti,Co)Ox coating

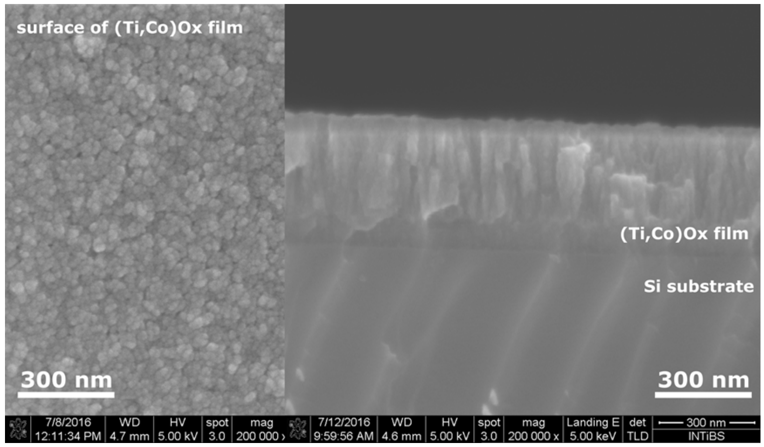


Fig. 2. SEM images of the surface and cross-section of the gradient (Ti,Co)Ox coating

In Fig. 3, the I-V characteristics of the gradient coating (Ti,Co)Ox measured in the transverse configuration (Au/(Ti,Co)Ox/Ti6Al4V) are shown. Note that positive voltage/current values are due to the forward bias condition of the prepared gradient structure, whereas negative values are due to the reverse bias condition. During the measurements, the current was forced from negative to positive values and then back from the applied positive current values to the negative ones, while the voltage drop was sensed using the source-measure unit (current-driven measurement). Sweeping the current allowed us to observe the hysteresis loop (Fig. 3a). The main conclusion that can be drawn from the I-V characteristics is the presence of a bipolar resistive switching effect, which is manifested by the mentioned pinched memory loop. The occurrence of such an effect in the case of $TiO_2$-based coatings with the addition of cobalt has been reported so far only in a few works [3,5,18]. However, in this case, we have obtained a resistive switching effect in a gradient thin film material, which is a novelty. The repeatability of this effect is also a great advantage of the prepared gradient coating. As can be seen in Fig. 3b, the hysteresis was still present even after 100 measurement cycles. This testifies that such gradient oxide coatings based on Ti and Co are prospective for optoelectronics and gives new possibilities for preparation of various electronic devices within the framework of transparent electronics.

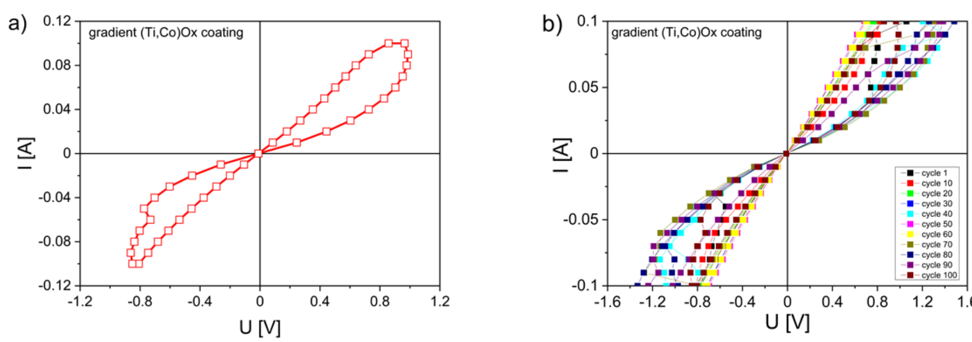


Fig. 3. I-V characteristics of the gradient (Ti,Co)Ox coating that exhibits a memristive effect (a) and its repeatability based on 100 measurement cycles (b).

The high attractiveness and potential possibilities offered by the application of the manufactured gradient coatings are also evidenced by the results of research on their optical properties. The transmission and reflection characteristics registered for normal incidence are presented in Fig. 4a. Also, in Fig. 4b the transmission characteristics (for S and P, measured at a 30 ° angle) are shown. These results demonstrate the high level of transparency of the prepared coating. Considering the high Co content in the entire volume of the coating, the transmission coefficient above 50% for the visible light range should be considered as a very good result. Based on the characteristics of $T_{\lambda}$, with the help of Scout modeling [27], the characteristics of the refractive index ($n$) and the extinction coefficient (k) were determined (Fig. 4c). Obtained values of refractive index are typical for oxide materials based on $TiO_2$, which is widely recognized as a high-$n$ material. For example, $n_{550}$ was equal to 2.14. In the case of extinction coefficient, obtained values (e.g. $k_{550}$ = 0.07) are 1-2 orders higher than for typical optical coatings, but it is also associated with a high cobalt content in the composition of the gradient coating. The influence of Co-additive can be observed in the band structure of the (Ti,Co)Ox film. Analysis with the aid of a Tauc plot (Fig. 4d) has shown that the optical band gap value ($E_g^{opt}$) was 1.61 eV. It was calculated from the $(\alpha h\nu)^{1/2}$ plot in the function of the photon energy (eV) [28,29]:

$$\alpha h\nu = \alpha_1 \left(h\nu - E_g^{\ opt}\right)^2 \quad (3.1)$$

where: h - Planck constant, $\nu$ - radiation frequency, $\alpha_1$ - constant coefficient.
Obtained value is about 2 times lower than for typical $TiO_2$ films [13,18,25] and is a consequence of a relatively high Co-content. It should also be noted that this effect can be considered as typical for $TiO_2$-based oxide materials with the addition of cobalt [18].

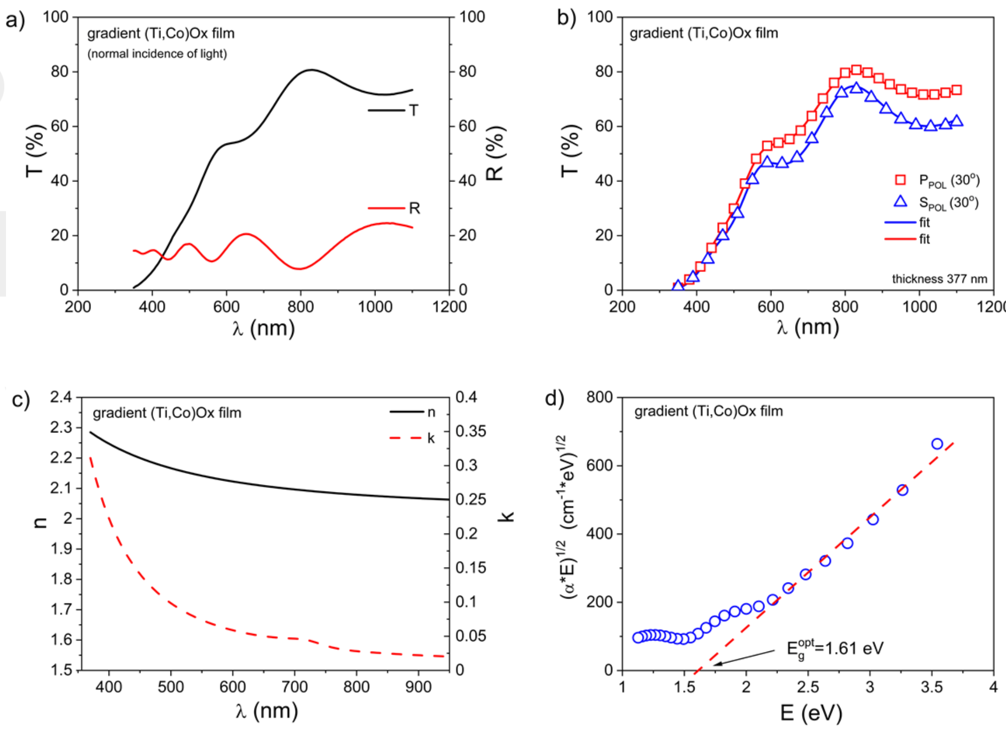


Fig. 4. Characteristics of transmission and reflection registered at normal incidence of light (a), transmission for polarization of S and P at 30° angle (b); with refractive index - $n$ and extinction coefficient - $k$ (c), and the Tauc plot (d) of the gradient (Ti,Co)Ox coating.

The gradient of cobalt concentration also had an effect on the structural properties of the coating. The results of the GIXRD measurements have shown that the as-deposited (Ti,Co)Ox film was amorphous (Fig. 5a). The effect of counteracting crystallization during the deposition of the sputtered material on the substrate probably occurred. We have already observed this impact of Co-additive in the case of $TiO_2$ coatings with its homogeneous distribution throughout the film volume [18]. The amorphous nature of the gradient layers was also investigated with the aid of Raman spectroscopy (Fig. 5b). The intensity of the peaks observed in the measured spectrum is very small, suggesting that the gradient coating is rather amorphous. However, as shown, very fine crystal forms of $TiO_2$-anatase and $Co_3O_4$ are present. The presence of $TiO_2$-anatase is indicated by the $E^A_g$ peak at 144 $cm^{-1}$ [30,31], while the presence of $Co_3O_4$ is suggested by the $F_{2g}$ and $A_{1g}$ peaks at 519 $cm^{-1}$ and 698 $cm^{-1}$, respectively [32-34]. Note that the Raman results did not give an unambiguous answer as to the amorphous or very fine crystalline structure of the (Ti,Co)Ox gradient film. Therefore, further studies were carried out using transmission electron microscopy.

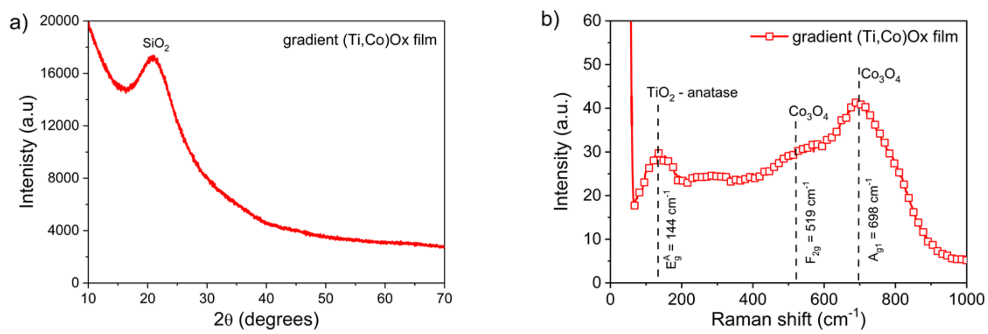


Fig. 5. GIXRD pattern (a) and Raman spectrum (b) of the gradient (Ti,Co)Ox coating as deposited on $SiO_2$

In Fig. 6 microstructure of gradient (Ti,Co)Ox coating can be observed on the cross section performed using the BFTEM, HRTEM and SAED techniques. The existence of a purely amorphous area was identified directly at the silicon substrate. It should be noted that the substrates were not heated prior to deposition; therefore, at the beginning of the nucleation the thin film remained amorphous. In turn, at a distance of approximately 50 nm from the substrate, when the amount of cobalt increased, the structure of the (Ti,Co)Ox coating was changed to fine nanocrystalline and densely packed, although much of the amorphous phase is still present (Fig. 6a,b). High-resolution images (HRTEM) were obtained to precisely determine the structure of the deposited gradient thin films and showed small crystallites with a size not exceeding 5 nm, which are located in a predominant amorphous surrounding (Fig. 6d-f). The HRTEM images with FFT (Fast Fourier Transform) diffraction patterns, taken from the crystallites free of defects, allowed for accurate evaluation of the plane separation values in three different parts of the thin films, i.e., at the substrate (Fig. 6d), in the middle (Fig. 6e) and at the surface (Fig. 6f) of the gradient coating. The HRTEM image at the substrate showed three areas of the crystalline silicon substrate, amorphous native silicon oxide, and amorphous (Ti,Co)Ox thin film. The other two images showed small nanocrystallites with marked (110) planes of $TiO_2$-anatase crystalline phase. The visible fringe spacings are equal to ca. 2.64 Å, which corresponds well to the separation between the (110) plane of the $TiO_2$-anatase phase. The selected area electron diffraction pattern (Fig. 6c) also showed rather fuzzy, broadened diffraction rings, which dominated over the rings with low intensity related to the highly nanocrystalline structure, testifying about the occurrence of the large volume of the amorphous phase in the thin film. However, three rings can be distinguished, which corresponded to the planes (200) and (110) of $TiO_2$-anatase and the plane (400) of the crystalline phases of $Co_3O_4$. This, in turn, confirmed the results obtained with the Raman spectroscopy measurements. The observed change of the microstructure character from amorphous to crystalline is combined with the increase in Co-content in the film. In Fig. 7 distribution of elements (linear scan across film thickness) with BFTEM of film cross section have been stacked together. On the basis of the linear approximation, two areas of gradient profile for Co can be distinguished. The first one from the Si substrate up to about 50 nm of layer thickness has a greater slope due to the higher sputtering rate of cobalt. In this region, as mentioned above, the layer is amorphous. In the rest, where the layer already has a fine crystalline structure, a smaller slope of the gradient profile can be noticed, which corresponds to a decrease in the sputtering rate. This effect is most likely related to the poisoning of the Co-target surface with oxygen, which was used as a reactive gas. As a result, an oxide was formed on its surface, which sputtering rate was not as effective as the metallic one [35,36].

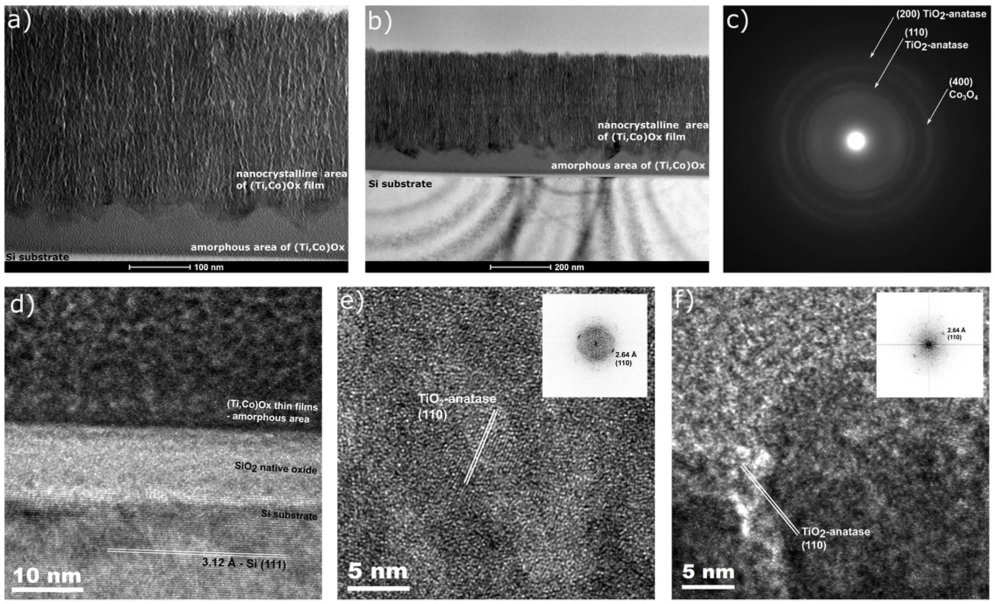


Fig. 6. Microstructure of the gradient (Ti,Co)Ox coating: BF TEM images of the cross section of the film (a,b); its SAED (c) with HRTEM images of the area near the Si substrate (d), in the middle (e) and at the top of the film (f)



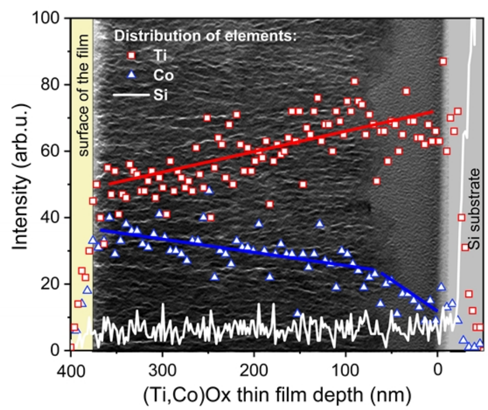


Fig. 7. BFTEM cross-section image of the gradient (Ti,Co)Ox coating with distribution of elements

## 4. Conclusions

This paper presents studies of oxide coatings based on a mixture of titanium and cobalt with gradient cobalt concentration. The prepared structure exhibits great potential as a transparent electronic device with resistance-switching effect. Such memory effects in transparent thin-film coatings open up new possibilities for the manufacturing of innovative memory elements in the future. Coatings were prepared by multi-magnetron sputtering and, despite the high cobalt content, were transparent and had a high refractive index. Gradient Co-addition resulted in the receipt of fine crystalline $TiO_2$ – anatase and $Co_3O_4$ forms in the amorphous surrounding. Observed resistance switching was a fully repeatable effect, and its occurrence in gradient (Ti,Co)Ox coatings was not reported earlier.

**Funding.** Polish National Science Centre (UMO-2018/29/B/ST8/00548; 2018-2022).

**Acknowledgments.** The authors thank Prof. Danuta Kaczmarek for a valuable discussion on the investigation results.

**Disclosures.** The authors declare no conflicts of interest.

**Data availability.** Data underlying the results presented in this article are not publicly available at this time, but may be obtained from the authors upon reasonable request.

## References

1. R. Ai, W. Luo, X. Liu, "Rectifier characteristics and analog bipolar resistive switching behavior in CoO-based memristor for artificial synapse application", Vacuum **188**, 110190 (2021).
2. J. Fu, M. Hua, S. Ding, X. Chen, R. Wu, S. Liu, J. Han, C. Wang, H. Du, Y. Yang, J. Yang, "Stability and its mechanism in Ag/CoOx/Ag interface-type resistive switching device", Sci. Rep. **6**, 35630 (2016).
3. D. Wojcieszak, J. Domaradzki, M. Mazur, T. Kotwica, D. Kaczmarek, "Investigation of a memory effect in a Au/(Ti–Cu)Ox-gradient thin film/TiAlV structure", Beilstein J. Nanotechnol. **13**, 265-273 (2022).
4. J. Domaradzki, D. Wojcieszak, T. Kotwica, E. Mankowska, "Memristors: A short review on fundamentals, structures, materials and applications", Int. J. Electron. Telecommun **66**, 373-381 (2020).
5. J. Domaradzki, T. Kotwica, M. Mazur, D. Kaczmarek, D. Wojcieszak, "Memristive properties of transparent oxide semiconducting (Ti,Cu)Ox-gradient thin film", Semicond. Sci. Technol. **33**, 015002 (2018).
6. H. Shima, F. Takano, H. Akinaga, Y. Tamai, I.H. Inque, H. Takagi, "Resistance switching in the metal deficient type oxides: NiO and CoO", Appl. Phys. Lett. **91**, 012901 (2007).
7. H. Shima, F. Takano, H. Muramatsu, H. Akinaga, Y. Tama, I.H. Inque, H. Takagi, "Voltage polarity dependent low-power and high-speed resistance switching in CoO resistance random access memory with Ta electrode", Appl. Phys. Lett. **93**, 113504 (2008).
8. A.A. Patil, S.S. Khot, R.U. Amate, P.N. Kamble, P.B. Patil, R.N. Bulakhe, I.In, T.D. Dongale, D. Kim, "Bipolar-resistive switching and memristive properties of solution processable cobalt oxide nanoparticles", J. Mat. Sci. – Mat. in Electr. **31**, 9695-9704 (2020).
9. Z.Q. Wang, X.H. Li, H.Y. Xu, W. Wang, H. Yu, X.T. Zhang, Y.X. Liu, Y.C. Liu, "Effects of compliance currents on the formation and rupture of conducting filaments in unipolar resistive switching of CoO film", J. Phys. D: Appl. Phys. **43**, 385105 (2010).
10. G. Chen, C. Song, F. Pan, "Improved resistive switching stability of Pt/ZnO/CoOx/ZnO/Pt structure for nonvolatile memory devices", Rare Met. **32(6)**, 544-549 (2013).
11. Z. Xu, M. Gao, L. Yu, L. Lu, X. Xu, Y. Jiang, "Co nanoparticles induced resistive switching and magnetism for the electrochemically deposited polypyrrole composite films", ACS Appl. Mater. Interfaces **6**, 17823-17830 (2014).
12. Z. Wang, Y. Sun, X. Zhou, F. Pan, C. Song, "Local control of exchange bias by resistive switching", Phys. Status Solidi **RRL**, 1800446 (2018).
13. M. Kitui, M.M. Mwamburi, F. Gaitho, M. Maghanga, "Optical properties of $TiO_2$ based multilayer thin films: Application to optical filters", Int. J. Thin Film. Sci. Technol. **4**, 17 (2015).
14. H.I. Elsaeedy, A. Qasem, H.A. Yakout, M. Mahmoud, "The pivotal role of $TiO_2$ layer thickness in optimizing the performance of $TiO_2$/P-Si solar cell", J. Alloy. Compd. **867**, 159150 (2021).
15. B. Lyson-Sypien, M. Radecka, M. Rekas, K. Swierczek, K. Michalow-Mauke, T. Graule, K. Zakrzewska, "Grain-size-dependent gas-sensing properties of $TiO_2$ nanomaterials", Sens. Actuators B Chem. **211**, 67-76 (2015).
16. J. Mei, T. Liao, G.A. Ayoko, J. Bell, Z. Sun, "Cobalt oxide-based nanoarchitectures for electrochemical energy applications", Prog. Mater. Sci. **103**, 596-677 (2019).
17. A.E. Kaloyeros, Y. Pan, J. Goff, B. Arkles, "Cobalt thin films: Trends in processing technologies and emerging applications", ECS J. Solid State Sci. Technol. **8**, P119 (2019).
18. D. Wojcieszak, M. Mazur, P. Pokora, A. Wrona, K. Bilewska, W. Kijaszek, T. Kotwica, W. Posadowski, J. Domaradzki, "Properties of metallic and oxide thin films based on Ti and Co prepared by magnetron sputtering from sintered targets with different Co-content", Materials **14**, 3797 (2021).
19. H.P. Quiroz, E.F. Galíndez, A. Dussan, "Ferromagnetic-like behavior of Co doped $TiO_2$ flexible thin films fabricated via co-sputtering for spintronic applications", Heliyon **6**, e03338 (2020).
20. N.M. Islam, J. Podder, "The role of Al and Co co-doping on the band gap tuning of $TiO_2$ thin films for applications in photovoltaic and optoelectronic devices", Mater. Sci. Semicond. Process. **121**, 105419 (2021).
21. P. Jiang, W. Xiang, J. Kuang, W. Liu, W. Cao, "Effect of cobalt doping on the electronic, optical and photocatalytic properties of $TiO_2$", Solid State Sci. **46**, 27-32 (2015).
22. M. Subramanian, S. Vijayalakshmi, S. Venkataraj, R. Jayavel, "Effect of cobalt doping on the structural and optical properties of $TiO_2$ films prepared by sol-gel process", TSF **516**, 3776 (2008).

23. D. Wojcieszak, M. Mazur, D. Gibson, G. Zatryb, D. Kaczmarek, J. Misiewicz, “Influence of europium on structure modification of $TiO_2$ thin films prepared by high energy magnetron sputtering process”, Surf. Coat. Tech. **320**, 132-137 (2017).

A. Obstarczyk, D. Kaczmarek, D. Wojcieszak, M. Mazur, J. Domaradzki, T. Kotwica, R. Pastuszek, D. Schmeisser, P. Mazur, M. Kot, “Tailoring optical and electrical properties of thin-film coatings based on mixed Hf and Ti oxides for optoelectronic application”, Mat. & Design **175**, art. 107822, 1-15 (2019).

24. A. Wiatrowski, M. Mazur, A. Obstarczyk, D. Wojcieszak, D. Kaczmarek, J. Morgiel, D. Gibson, “Comparison of the physicochemical properties of $TiO_2$ thin films obtained by magnetron sputtering with continuous and pulsed gas flow”, Coatings **8**, 412 (2018).

25. A. Wiatrowski, M. Mazur, A. Obstarczyk, D. Kaczmarek, R. Pastuszek, D. Wojcieszak, M. Grobelny, M. Kalisz, “Influence of magnetron powering mode on various properties of $TiO_2$ thin films”, Mater. Sci. Pol. **36**, 748-760 (2018).

26. M.-B. Bouzourâa, A. En Naciri, Y. Battie, S. Dalmasso, S. Diliberto, A. Bouché, N. Chaoui, “Correlation between optical and structural properties of nitrogen doped anatase $TiO_2$ thin films”, Opt. Mat. **133**, 112919 (2022).

27. W. Theiss, SCOUT ver. 4.17, www.mtheiss.com

28. K. Kollbek, M. Sikora, Cz. Kapusta, J. Szlachetko, K. Zakrzewska, K. Kowalski, M. Radecka, “X-ray spectroscopic methods in the studies of nonstoichiometric $TiO_{2-x}$ thin films”, Appl. Surf. Sci. **281**, 100-104 (2013).

29. P. Makuła, M. Pacia, W. Macyk, “How to correctly determine the band gap energy of modified semiconductor photocatalysts based on UV–Vis spectra”, J. Phys. Chem. Lett. **9 (23)**, 6814-6817, (2018).

30. J.J. Jasinski, M. Lubas, K. Suchorab, M. Gawęda, L. Kurpaska, M. Brykala, A. Kosinska, M. Sitarz, J. Jagielski, “Qualitative and semi-quantitative phase analysis of $TiO_2$ thin layers by Raman imaging, J. Mol. Str. **1260**, 132803 (2022).

31. T.G. Vo, P.Y. Ho, C.Y. Chiang, “Operando mechanistic studies of selective oxidation of glycerol to dihydroxyacetone over amorphous cobalt oxide”, Appl. Cat. B - Env. **300** 120723 (2022).

32. V.G. Hadjiev, M.N. Iliev, I.V. Vergilov, “The Raman spectra of $Co_3O_4$”, J. Phys. C Solid State Phys. **21** L199-L201 (1988).

33. J. Yang, H. Liu, W.N. Martens, R.L. Frost, “Synthesis and characterization of cobalt hydroxide, cobalt oxyhydroxide, and cobalt oxide nanodiscs”, J. Phys. Chem. C **114** 111-119 (2010).

34. B.-S. Lou, W.-T. Chen, W. Diyatmika, J.-H. Lu, C.-T. Chang, P.-W. Chen, J.-W. Lee, “Effect of target poisoning ratios on the fabrication of titanium oxide coatings using superimposed high power impulse and medium frequency magnetron sputtering”, Surf. Coat. Technol. **421**, 27430 (2021).

35. A. Brudnik, H. Czternastek, K. Zakrzewska, M. Jachimowski, “Plasma-emission-controlled d.c. magnetron sputtering of $TiO_{2-x}$ thin films”, TSF **199(1)**, 45-58 (1991).